PB82-205865

Interferogram-Based Infrared Search System

(U.S.) Environmental Research Lab.
Athens, GA

1981

U.S. Department of Commerce
National Technical Information Service
NTIS

TECHNICAL REPORT DATA
(Please read Instructions on the reverse before completing)

1. REPORT NO. EPA-600/J-81-548	2. Journal Article	3 PB82-205865
4. TITLE AND SUBTITLE Interferogram-Based Infrared Search System		5. REPORT DATE May 1982 6. PERFORMING ORGANIZATION CODE
7. AUTHOR(S) James A. de Haseth and Leo V. Azarraga*		8. PERFORMING ORGANIZATION REPORT NO.
9. PERFORMING ORGANIZATION NAME AND ADDRESS University of Alabama, University, Alabama 35486; *Environmental Research Laboratory, USEPA, Athens GA 30613		10. PROGRAM ELEMENT NO. CBNC1A 11. CONTRACT/GRANT NO.
12. SPONSORING AGENCY NAME AND ADDRESS U.S. Environmental Protection Agency--Athens GA, Environmental Research Laboratory, College Station Road, Athens GA 30613		13. TYPE OF REPORT AND PERIOD COVERED Journal Article 14. SPONSORING AGENCY CODE EPA/600/01

15. SUPPLEMENTARY NOTES
Analytical Chemistry. 53(14):2292-2296, 1981
Contact: L.V. Azarraga, 8-250-3552

16. ABSTRACT

A computerized search routine for the identification of infrared spectra using interferometric data exclusively is described. Two forms of instrument-dependent information present in raw interferometric data are removed prior to the search process. Interferometric phase error is removed by a convolution process. The instrument function is eliminated by vector subtraction. The search routine was applied to several target compounds using a collection of 3300 infrared vapor-phase interferograms maintained at the U.S. Environmental Protection Agency's Environmental Research Laboratory in Athens, GA. Even by using a primitive matching algorithm for searching "unknowns" within the library, excellent results were obtained. In all cases the target compounds were perfectly matched, as expected for an internal library search; however, all the nonexact matches were well distinguished from the exact match and in all cases were structurally similar to the target compound. The capability to locate erroneous entries in the library is demonstrated.

17. KEY WORDS AND DOCUMENT ANALYSIS

a. DESCRIPTORS	b. IDENTIFIERS/OPEN ENDED TERMS	c. COSATI Field/Group

REPRODUCED BY
NATIONAL TECHNICAL
INFORMATION SERVICE
U.S. DEPARTMENT OF COMMERCE
SPRINGFIELD, VA 22161

18. DISTRIBUTION STATEMENT RELEASE TO PUBLIC	19. SECURITY CLASS *(This Report)* UNCLASSIFIED	21. NO. OF PAGES 7
	20. SECURITY CLASS *(This page)* UNCLASSIFIED	22. PRICE

EPA Form 2220-1 (9-73)

EPA-600/J-81-548
Journal Article

Interferogram-Based Infrared Search System

James A. de Haseth*

Department of Chemistry, University of Alabama, University, Alabama 35486

Leo V. Azarraga

Environmental Research Laboratory, U.S. Environmental Protection Agency, Athens, Georgia 30613

A computerized search routine for the identification of infrared spectra using interferometric data exclusively is described. Two forms of instrument-dependent information present in raw interferometric data are removed prior to the search process. Interferometer phase error is removed by a convolution process. The instrument function is eliminated by vector subtraction. The search routine was applied to several target compounds using a collection of 3300 infrared vapor-phase interferograms maintained at the U.S. Environmental Protection Agency's Environmental Research Laboratory in Athens, GA. Even by using a primitive matching algorithm for searching "unknowns" within the library, excellent results were obtained. In all cases the target compounds were perfectly matched, as expected for an internal library search; however, all the nonexact matches were well distinguished from the exact match and in all cases were structurally similar to the target compound. The capability to locate erroneous entries in the library is demonstrated.

The necessity for spectral search routines to aid the analyst in the interpretation of unknown spectra has been well established. Many search systems have been devised for infrared spectra, but only recently has the practical application of gas chromatography–infrared spectrometry (GC-IR) and computerized data systems generated substantial interest in reliable, rapid search procedures. Emphasis has been upon search methods that use spectral or frequency-mode representations of the data. These methods have been quite successful; however, it is difficult to encode spectral information in a concise manner. Peak position, intensity, band shape, and peak width data in spectra comprise a large amount of information. It is difficult to store this information concisely in a small data record of, for example, 100 computer words. As most search routines use sequential data acquisition, the library data entry size must be minimized so as to speed the search. Thus one has a dichotomy: in order to have a rapid search the data entries must be small, but to appropriately encode the spectral information large amounts of information must be stored per entry. In general, the accuracy of the search diminishes as the information per entry is reduced; thus, much effort is expended determining optimum data storage as well as developing efficient matching algorithms.

One method of effectively compressing a spectrum is to take the Fourier transform of the spectral representation to obtain a time (or distance) domain representation. Fellgett (*1*) showed that each datum of the time domain representation contains information about every frequency in the spectrum. Furthermore, it is known that the resolution of the spectral representation depends upon the size of the time domain representation; that is, the longer the interferogram, the higher the resolution of the spectrum. Thus, a short interferogram is equivalent to a low-resolution spectrum and the interferogram has all peak position, intensity, band shape, and peak width information of the spectrum.

GC-IR data are usually collected with a Fourier transform infrared spectrometer (FT-IR) and the data collected are in the time or distance domain, i.e., interferograms. Therefore, it would appear straightforward to use the interferometric data directly for infrared searches. The data are initially in a compressed format, and all the spectral information is in the interferogram. The usefulness of interferometric data has been demonstrated previously by the implementation of a gas chromatographic reconstruction algorithm (*2*). Direct interferometric search systems have been proposed (*3*) and at least one attempt has been made to perform such a search (*4*). Although the previously described direct interferogram search was computationally efficient, the results were not sufficiently reliable for it to be used as a routine search method. A new approach is presented by which a direct interferogram-based search is performed and the search reliability is shown to be extremely high.

THEORY

The primary objective of any search system is to utilize data that are instrument independent. Unfortunately, the concept of instrument independent spectra is a limited assumption. Spectra are dependent upon at least, the bandwidth of the spectrometer, the instrument line shape, the responsiveness of the detector, the dynamic range of the recording apparatus, and the sampling frequency of the spectrometer. All these parameters are inherent to any instrument, either interference or dispersive, and will prevent perfect spectroscopic independence. In the spectral mode, an absorbance spectrum is considered to be instrument independent and is used often for searches. The absorbance spectrum can be inverse Fourier transformed to produce a time domain, spectrometer-independent signal. Of course, this signal is easily calculated from the absorbance spectrum, but a direct interferogram approach is lost. It is not a straightforward operation to calculate an inverse Fourier transform of an absorbance spectrum without going through a Fourier transform; therefore, an alternate instrument independent data representation must be found.

A spectrometer-dependent feature of FT-IR spectra is phase error, which distorts spectral bands and base lines. Phase error, commonly called chirping, is produced by asymmetry in the interferogram. The primary causes of phase error may be found in the frequency-dependent dispersive qualities of the beamsplitter (particularly the support medium for the dielectric beamsplitter film), the sampling of the interferogram, and the recording electronics. In addition, any misalignment in the Michelson interferometer may further add to the phase error (*5*). Two basic methods are used to remove the phase error from a spectrum: one was developed by Mertz and is done in the spectral domain (*6*); the other by Forman et al. is performed on the interferogram (*7*). As a direct interferometric approach was sought for this study, the method of Forman et al. was adopted.

In a two-beam interferometer, such as the Michelson interferometer, an interferogram $I'(\delta)$ is recorded and can be

transformed to a spectrum $B'(\bar{\nu})$. Thus

$$B'(\bar{\nu}) = \int_{-\infty}^{\infty} I'(\delta) e^{i2\pi\bar{\nu}\delta}\, d\delta \quad (1)$$

where δ is the optical path difference (retardation) between the two arms of the interferometer and $\bar{\nu}$ is the spectral frequency in wavenumbers. [It is customary to represent a Fourier transform as the transformation from the time (t, s) to the frequency domain (ν or, f, Hz). Equation 1 is equivalent to this convention as δ can be converted to t by division by the speed of light, c, and $\bar{\nu}$ can be converted to ν by multiplication by c.] If the Fourier transform of eq 1 is performed, $B'(\bar{\nu})$ is found to be the complex function

$$B'(\bar{\nu}) = \mathrm{Re}(\bar{\nu}) + i\mathrm{Im}(\bar{\nu}) \quad (2)$$

where $\mathrm{Re}(\bar{\nu})$ and $\mathrm{Im}(\bar{\nu})$ are the real and imaginary parts of $B'(\bar{\nu})$, respectively. Equation 2 is one form of the Fourier transform and may also be expressed as

$$B'(\bar{\nu}) = |B(\bar{\nu})| e^{i\phi(\bar{\nu})} \quad (3)$$

where

$$|B(\bar{\nu})| = \{[\mathrm{Re}(\bar{\nu})]^2 + [\mathrm{Im}(\bar{\nu})]^2\}^{1/2} \quad (4)$$

and is called the amplitude or power spectrum. Also

$$\phi(\bar{\nu}) = \arctan [\mathrm{Im}(\bar{\nu})/\mathrm{Re}(\bar{\nu})] \quad (5)$$

where $\phi(\bar{\nu})$ is the phase of the function $B'(\bar{\nu})$.

The true spectrum, $B(\bar{\nu})$, is not equal to $|B(\bar{\nu})|$ except in an ideal situation. In practice $I'(\delta)$ includes signal noise, which is present in its Fourier transform. By calculating the amplitude spectrum $|B(\bar{\nu})|$ as indicated by eq 4, all the noise is positive. This has a nonlinear effect on the signal-to-noise ratio and does not accurately represent the true spectrum $B(\bar{\nu})$.

As indicated above, the phase error $\phi(\bar{\nu})$ can arise from various sources. The effect of phase error is to skew the base line of $B'(\bar{\nu})$ and distort the absorption bands. This distortion can be quite severe and bands may be shifted and have erroneous absorption intensities. In an ideal interferometer, the phase error is zero at all frequencies and $B'(\bar{\nu}) = |B(\bar{\nu})|$. If the phase error is zero, $\mathrm{Im}(\bar{\nu})$ must be zero and $B(\bar{\nu}) = \mathrm{Re}(\bar{\nu})$. If the Fourier transform of the interferogram is calculated and the imaginary portion of the spectrum is zero, then $B'(\bar{\nu})$ will have no nonlinear errors and will be photometrically accurate. Hence, from eq 2, 3, and 4

$$\begin{aligned} B'(\bar{\nu}) e^{-i\phi(\bar{\nu})} &= B(\bar{\nu}) \\ &= \mathrm{Re}(\bar{\nu}) \end{aligned} \quad (6)$$

Equation 6 implies that the true spectrum $B(\bar{\nu})$ can be calculated from the Fourier transform of $I'(\delta)$ multiplied by the inverse of the complex phase error, $e^{-i\phi(\bar{\nu})}$. When this procedure is carried out in the spectral or frequency domain, it is the method devised by Mertz (6).

This operation can also be carried out in the interferogram or time domain. It is a known property of Fourier mathematics that multiplication in one domain is equivalent to convolution in the other. Prior to performing the convolution, however, it is first necessary to compute the inverse Fourier transform of $B'(\bar{\nu})$ and $e^{-i\phi(\bar{\nu})}$. By eq 1 and the existence of Fourier transform pairs, it follows that

$$I'(\delta) = \int_{-\infty}^{\infty} B'(\bar{\nu}) e^{i2\pi\bar{\nu}\delta}\, d\bar{\nu} \quad (7)$$

similarly

$$\Phi(\delta) = \int_{-\infty}^{\infty} e^{-i\phi(\bar{\nu})} e^{i2\pi\bar{\nu}\delta}\, d\bar{\nu} \quad (8)$$

Thus the phase corrected interferogram is then

$$\begin{aligned} I(\delta) &= \int_{-\infty}^{\infty} I'(\delta')\Phi(\delta - \delta')\, d\delta \\ &= I'(\delta) * \Phi(\delta) \end{aligned} \quad (9)$$

where * denotes convolution.

After convolution, $I(\delta)$ has zero phase error and the imaginary portion of Fourier transform is equal to zero. $I(\delta)$ is a real and even function and is symmetric about zero optical retardation. For computation, only half of the interferogram is transformed. The signal from zero to infinity is transformed by a cosine Fourier transform as there is no sine or imaginary character to the interferogram.

In practice, the phase error is smooth and continuous and essentially varies only slowly with frequency. Consequently the phase error can be well characterized by a few data points, that is, a small interferogram. $\Phi(\bar{\nu})$ is calculated from a short two-sided interferogram, typically 128 or 256 points. The convolution of $\Phi(\delta)$ and $I'(\delta)$ is computationally much more efficient if the size of $\Phi(\delta)$ is reduced to a minimum.

EXPERIMENTAL SECTION

Computations were carried out on a Nova 3/12 minicomputer with 128 kbytes of memory and a 10 Mbyte moving-head disk. The minicomputer system is part of a Digilab FTS-14/C/D Fourier transform infrared spectrometer. Some computations were too time-consuming to be completed on the minicomputer system and these were executed on a Univac 1100/61 mainframe system with 1 048 576 words (36 bits/word) of high-speed memory.

The data used were from the collection of 3300 vapor-phase infrared spectra collected by the U.S. Environmental Protection Agency, Athens Environmental Research Laboratory (EPA/AERL), Athens, GA. These spectra comply with the format specified by the Coblentz Society (8).

Programs were written for the phase correction of all 6600 interferograms (one sample and one reference per entry in the EPA/AERL vapor-phase spectral library). All programs were written in FORTRAN except for one assembler language subroutine.

RESULTS AND DISCUSSION

It was established earlier (2) that a region of high information content in an interferogram lies near the centerburst. This region apparently contains sufficient information to characterize the spectrum and the remaining data in the interferogram are not required. Consequently phase correction need not be carried out on the entire interferogram. Each interferogram entry in the EPA/AERL data base was truncated to the first 700 data points. This region always contained the centerburst and was of a sufficient size to prosecute the phase correction. A 256-data-point interferogram, sampled symmetrically about the centerburst, was used to calculate the phase error. The inverse Fourier transform of the phase error was convolved with the 700-point interferogram by the method discussed above. The effectiveness of the convolution method can be seen in Figure 1. Figure 1a illustrates a typical interferogram as found in the vapor-phase spectral library. This interferogram is highly chirped and exhibits a large amount of spectrometer sampling information. Figure 1b is the result of the phase correction operation after it was performed on Figure 1a. Almost all the phase error has been removed, as is indicated by the near ideal symmetry of this interferogram. In practice, the phase correction method does not eliminate all the phase error with a single convolution, but unless the interferogram is extremely asymmetric, a single correction reduces the phase to almost nil. The phase correction procedure was performed on all 6600 sample and reference interferograms in the collection using a mainframe computer. The total computation time was about 6 h, but it should be noted that it was necessary to perform this computation only once.

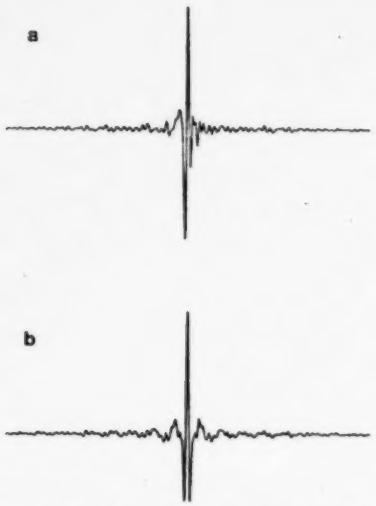

Figure 1. A sample interferogram as extracted from the EPA/AERL collection (a) and after it has been phase corrected (b).

Although the phase error was removed from all the sample and reference interferogram entries, the data were by no means instrument independent. The spectrometer instrument function was still present in each interferogram. In the spectral domain, the instrument function is removed by dividing the sample spectrum by the appropriate reference spectrum. This quotient produces a transmittance spectrum that is often further processed to give the absorbance spectrum. The mathematical procedure necessary to produce an inverse Fourier transform of an absorbance spectrum, without calculating the absorbance spectrum, is quite involved and may not even be desirable. Of course, the inverse Fourier transform of an absorbance spectrum may be taken; however, this defeats the objective of producing and using data directly in the time domain. An alternate method of calculating an instrument-independent interferogram is to perform a vector subtraction between sample and reference interferograms. One computationally efficient method by which a vector subtraction can be performed is the Gram–Schmidt vector orthogonalization method.

It was shown in an earlier publication (2) that the Gram–Schmidt method was useful for the direct reconstruction of GC/FT-IR chromatograms from the interferometric data. The reconstruction process required only a 100-point vector, selected from a region displaced approximately 60 points from the centerburst of the interferogram. A similar procedure was followed in this search system.

The vector orthogonalization algorithm produces interferogram patterns that are distinctive for the sample. To be successful for identification purposes, the phase error must be eliminated. By way of example, a Gram–Schmidt orthogonalization was performed on a sample/reference interferogram pair for phase corrected and uncorrected interferogram data. Figure 2a shows the Gram–Schmidt orthogonalization of a toluene sample interferogram and its respective reference interferogram, both of which have not been phase corrected. Although a distinctive pattern is seen in the resultant data, it is not symmetric. When a pattern such as the one illustrated in Figure 2a is used in a search system, the phase is encoded with the entry. Phase is spectrometer-dependent and hence becomes noise with respect to the true signal. Any search that includes the phase is automatically degraded as the phase will change from spectrometer to spectrometer, and with time in a given spectrometer.

Figure 2b is the same sample, but after both interferograms have been phase corrected. The pattern is symmetric and

Table I. Search Results for Toluene

Test Compound: Toluene

Hit No.	Dot Product	Name	Structure
1.	1.0000	Toluene	
2.	0.9341	1,2-Diphenylethylamine	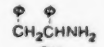
3.	0.9221	3-Methylbiphenyl	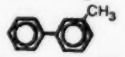
4.	0.9129	Bibenzyl	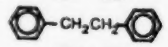
5.	0.9114	4-Methylbiphenyl	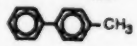

Table II. Search Results for Anisole

Test Compound: Anisole

Hit No.	Dot Product	Name	Structure
1.	1.0000	Anisole	
2.	0.9679	(2-Chloroethyl) phenyl ether	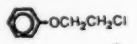
3.	0.9667	1,2-Epoxy-3-phenoxypropane	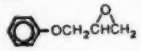
4.	0.9547	Phenylpropyl ether	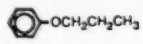
5.	0.9507	o-Methoxybenzyl alcohol	

Table III. Search Results for Acetone

Test Compound: Acetone

Hit No.	Dot Product	Name	Structure
1.	1.0000	Acetone	
2.	0.9980	m-Methylphenetole	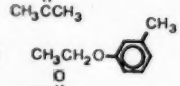
3.	0.9502	Chloroacetone	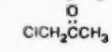
4.	0.9163	Diethylaminoacetone	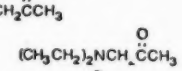
5.	0.9097	Phenyl-2-propanone	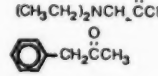

visually distinctive. For comparison Figure 3 has four additional interferogram patterns, ethylbenzene, *m*-dichlorobenzene, phenol, and acetone. Including toluene, four of the five compounds are aromatic. Even though it can be clearly recognized that these patterns are distinctively different, similarities among the aromatics can be found. Acetone, being aliphatic, has a pattern that departs drastically from the aromatics. It is clearly apparent that the centerburst is missing in all these patterns. This indicates that the centerburst contains little information as it is almost totally removed upon vector subtraction.

As indicated above, the entire pattern was not required for identification. Only a 100-point segment of the instrument-independent interferogram was required. Specifically, a 100-point segment of consecutive data points, with the first datum in the segment displaced 60 data points away from and to the right of the centerburst, was extracted from all 3300 entries in the EPA/AERL collection to form a search library. These entries became the basis of the interferometric search system.

To test the potential of such a library for searching purposes, we devised an internal search. Library entries were selected at random as "unknown" compounds and matched

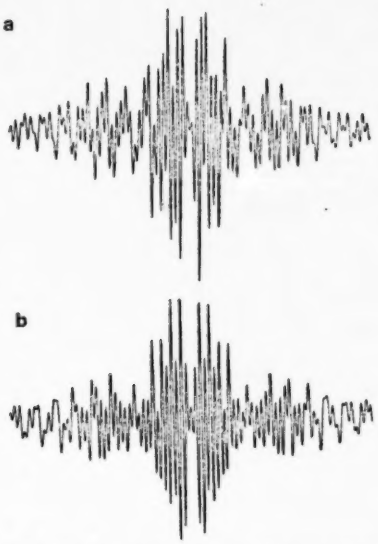

Figure 2. Comparison between two Gram–Schmidt patterns for toluene: (a) without any phase correction, (b) phase corrected.

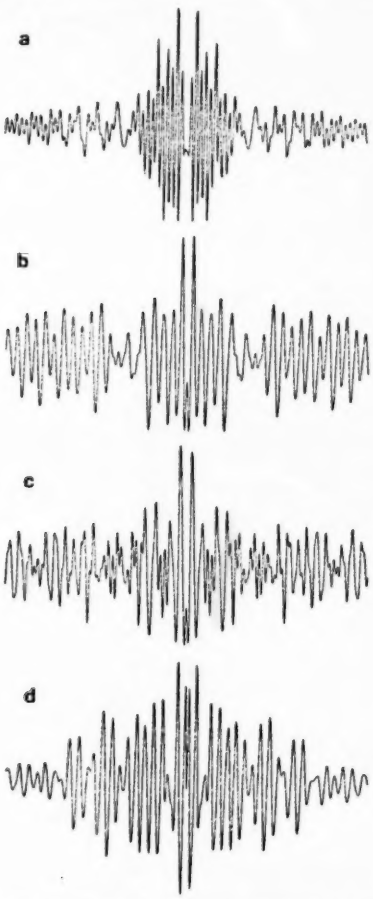

Figure 3. Gram–Schmidt interferogram patterns for (a) ethylbenzene, (b) *m*-dichlorobenzene, (c) phenol, and (d) acetone.

to the library data base. The matching algorithm is a simple dot product between the unknown and library entries. A perfect match for a dot product measurement has the value of unity and a complete mismatch has negative values or zero. The closeness of exact match is measured by the dot product as it approaches unity. Tables I–III present the results of three

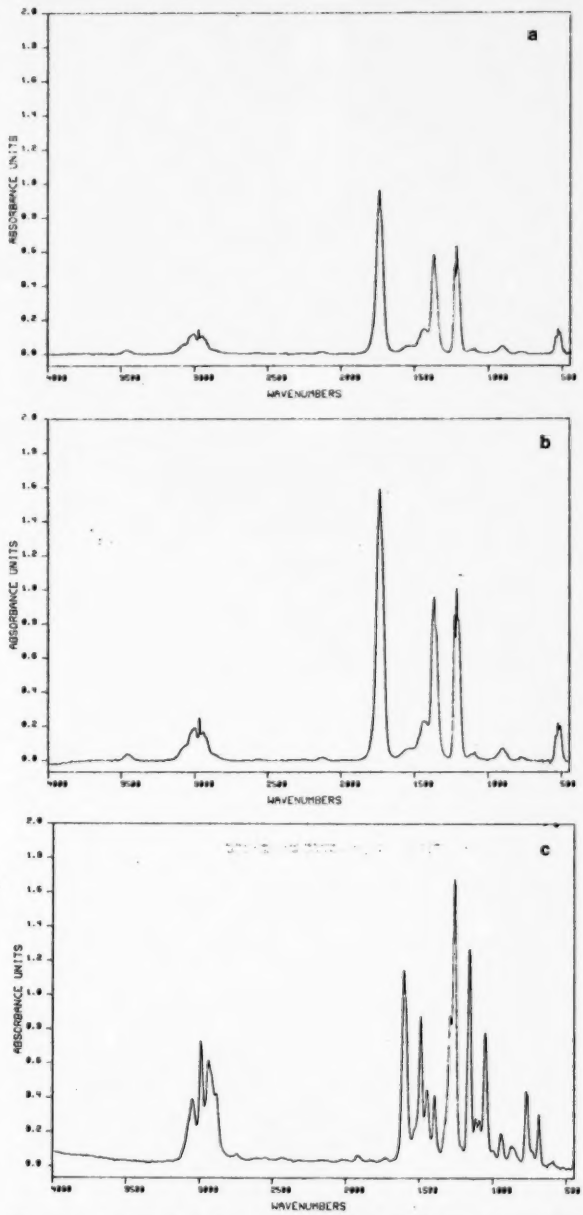

Figure 4. Investigation of search results from Table III: (a) spectrum of the interferogram for the *m*-methylphenetole entry, (b) spectrum of acetone, and (c) the spectrum of *m*-methylphenetole.

such test searches. In all cases the "unknown" is matched perfectly, as expected, because the test and library entries in these cases are exactly the same. Table I is the test run for toluene. The closest nonexact match is 1,2-diphenylethylamine, which has functional groups quite similar to those in toluene. All the other close matches had similar chemical moieties. Of note is that the closest match to the unknown, excluding the exact match, has a dot product of 0.93 and is different from unity by seven parts per hundred. The results presented in Table II, a search for anisole, parallel those of Table I. The closest nonexact match to anisole is another aliphatic phenyl ether and is differentiated from the exact match by over 3%. The results from Table III are consistent with those in Tables I and II except that the closest nonexact match, *m*-methylphenetole, is different from acetone by only 2 ppt. Examination of the transform of the interferogram for this library entry yielded the spectrum of acetone. The

spectrum of the interferogram for the *m*-methylphenetole entry is shown in Figure 4a. Figure 4b is the spectrum of acetone, and the spectrum of *m*-methylphenetole is presented in Figure 4c. In this case, an error in the data set was located, rather than a failure of the search system.

CONCLUSIONS

A functional interferogram search system was clearly demonstrated. Several assumptions were made in the demonstration of the system. The primary assumption was that dependent features of the data do not interfere with the search. These features include, sampling interval, instrumental band shape, bandwidth, inherent dynamic range, and detector responsiveness. This assumption is not precisely true. The data base spectra have a bandwidth of approximately 4000 wavenumbers (i.e., 450–4500 cm^{-1}) because the spectra were collected with a TGS detector. In practical GC/FT-IR applications, an MCT detector that covers the bandwidth of approximately 750–2800 wavenumbers is used. Interferogram patterns from these two detectors are incompatible due to the different bandwidths of the detectors. Work is continuing to correct this incompatibility and demonstrate the system with GC/FT-IR data. Nevertheless, a viable, workable interferometric search system has been demonstrated and the need for instrument-independent interferometric data has been clearly defined.

LITERATURE CITED

(1) Fellgett, P. B. *J. Phys. Radium* **1958**, *19*, 187–237.
(2) de Haseth, J. A.; Isenhour, T. L. *Anal. Chem.* **1977**, *49*, 1977–1981.
(3) de Haseth, James A. Ph.D. Dissertation, University of North Carolina at Chapel Hill, 1977.
(4) Small, G. W.; Rasmussen, G. T.; Isenhour, T. L. *Appl. Spectrosc.* **1979**, *33*, 444–450.
(5) Schroder, B.; Geick, R. *Infrared Phys.* **1978**, *18*, 595–605.
(6) Mertz, L. *Infrared Phys.* **1967**, *7*, 17–23.
(7) Forman, Michael L.; Steel, W. Howard; Vanasse, George A. *J. Opt. Soc. Am.* **1966**, *56*, 59–63.
(8) Griffiths, Peter R.; Azarraga, Leo V.; de Haseth, James; Hannah, Robert W.; Jakobsen, Robert J.; Ennis, Margaret M. *Appl. Spectrosc.* **1979**, *33*, 543–548.

RECEIVED for review July 17, 1981. Accepted September 18, 1981. Mention of trade names or commercial products does not constitute endorsement or recommendation for use by the U.S. Environmental Protection Agency. Financial support for J.A.deH. by the U.S. Environmental Protection Agency under Cooperative Agreement CR807302010 is greatly appreciated. This work was presented in part at the Pittsburgh Conference on Analytical Chemistry and Applied Spectroscopy, Atlantic City, NJ, March 1981.

Some Cation and Anion Attachment Reactions in Laser Desorption Mass Spectrometry

K. Balasanmugam, Tuan Anh Dang, R. J. Day, and David M. Hercules*

Department of Chemistry, University of Pittsburgh, Pittsburgh, Pennsylvania 15260

Positive- and negative-ion laser desorption mass spectra reveal cationization by metals and anionization by chloride. Cationized molecules can be detected in the absence of protonated molecules and metal-containing fragment ions are sometimes observed. Chloride ion attachment to pyridoxamine and pyridoxine occurs when their hydrochloride salts are subjected to laser irradiation. These ion attachment processes are analogous to those observed in other forms of desorption ionization.

In recent years significant progress has been made toward obtaining mass spectra of involatile organic compounds. Crucial to this effort has been the exploitation of new ionization methods such as field desorption (FD) (*1*, *2*) laser desorption (LD) (*3–8*), secondary ion mass spectrometry (SIMS) (*9–13*) and the related fast atom bombardment (FAB) techniques (*14*), electrohydrodynamic ionization (EHD) (*15–17*), and ^{252}Cf-plasma desorption (PD) (*18–20*).

A common characteristic of these techniques is the generation of cationized species in which a metal cation, usually Na or K, becomes attached to the intact sample molecule. Although alkali cations present as impurities are often sufficient to cationize samples using these ionization methods, results are sometimes obtained after the addition of a metal salt to the sample (*10*, *13*, *21*, *22*). Cationization reactions occurring during SIMS have been studied and are known to be general in nature; alkali, transition, and main-group metals have all been observed to cationize organic molecules (*10*, *22*). Cation attachment reactions are also initiated by laser desorption, as evidenced by the detection of $(M + Na)^+$ ions for a variety of samples including the carbohydrate stachyose (*3*). Indeed, in many cases cationization is critical to the observation of intact molecular species for involatile and thermally labile samples, $(M + H)^+$ typically being absent.

Recent experiments have shown that alkali cationized molecules can be generated simply by heating (*23*, *24*). Studies of $(M + Na)^+$ formation in LD have suggested that cationized species arise by attachment of thermally emitted Na^+ ions to desorbed organic molecules (*6*). In addition, silver attachment to sucrose has been reported by LD (*7*). Heavy metals such as Sb can attach to organics in EHD. The observation of $(M + C)^+$ ions, C = cation, for these various techniques suggests that the ion attachment processes initiated by all the desorption ionization methods are similar. In fact, the same mechanism has been proposed to account for cation attachment in several of these methods: metal ion formation followed by formation and emission of the metal–molecule complex (*6*, *10*, *13*). The present report describes further results on metal attachment reactions in LD. The analogous anion attachment process, anionization, has been reported for field desorption (*2*), electrohydrodynamic ionization (*15–17*), and PD (*19*). We have also observed attachment of chloride ions in LD. The purpose of the present communication is to show that attachment reactions are general in LD both with regard to organic types and for different metal ions.

EXPERIMENTAL SECTION

LD mass spectra were obtained by using commercially available instrumentation (Leybold-Heraeus LAMMA 500). The output

0003-2700/81/0353-2296$01.25/0 © 1981 American Chemical Society